Clinical Chemistry 51:1
47–55 (2005)

Proteomics and
Protein Markers

Protein Chip Array Profiling Analysis in Patients with Severe Acute Respiratory Syndrome Identified Serum Amyloid A Protein as a Biomarker Potentially Useful in Monitoring the Extent of Pneumonia

Timothy T.C. Yip,[1†] Johnny W.M. Chan,[2†] William C.S. Cho,[1] Tai-Tung Yip,[3] Zheng Wang,[3] Ting-Lok Kwan,[4] Stephen C.K. Law,[1*] Dominic N.C. Tsang,[5] John K.C. Chan,[5] King-Chung Lee,[5] Wai-Wai Cheng,[1] Victor W.S. Ma,[1] Christine Yip,[3] Cadmon K.P. Lim,[1] Roger K.C. Ngan,[1] Joseph S.K. Au,[1] Angel Chan,[5] Wilina W.L. Lim,[6] and Queen Elizabeth Hospital/Hong Kong Government Virus Unit/Ciphergen SARS Proteomics Study Group[7]

Background: **A new strain of coronavirus (CoV) has caused an outbreak of severe acute respiratory syndrome (SARS), with 8098 individuals being infected and 774 deaths worldwide. We carried out protein chip array profiling analysis in an attempt to identify biomarkers that might be useful in monitoring the clinical course of SARS patients.**

Methods: **We performed surface-enhanced laser desorption ionization time-of-flight mass spectrometry on 89 sera collected from 28 SARS patients, 72 sera from 51 control patients with various viral or bacterial infections, and 10 sera from apparently healthy individuals.**

Results: **Nine significantly increased and three significantly decreased serum biomarkers were discovered in the SARS patients compared with the controls. Among these biomarkers, one (11 695 Da) was identified to be serum amyloid A (SAA) protein by peptide mapping and tandem mass spectrometric analysis. When we monitored the SAA concentrations longitudinally in 45 sera from four SARS patients, we found a good correlation of SAA concentration with the extent of pneumonia as assessed by a serial chest x-ray opacity score. Increased SAA occurred in three of four patients at the time of extensive pneumonia as indicated by high x-ray scores. Over the course of gradual recovery in two patients, as assessed clinically and radiologically, SAA concentrations gradually decreased. In the third patient, the concentrations were initially increased, but were further increased with superimposed multiple bacterial infections. SAA was not markedly increased in the fourth patient, who had low x-ray scores and whose clinical course was relatively mild.**

Conclusions: **Protein chip array profiling analysis could be potentially useful in monitoring the severity of disease in SARS patients.**

A new strain of coronavirus (CoV)[8] caused a pandemic outbreak of severe acute respiratory syndrome (SARS) in mainland China, Hong Kong, Singapore, Toronto, and Taiwan during 2002 and 2003, with 8098 individuals

Departments of [1] Clinical Oncology, [2] Medicine, [4] Diagnostic Radiology, and [5] Pathology, Queen Elizabeth Hospital, Hong Kong Special Administrative Region, The People's Republic of China.

[3] Ciphergen Biosystems Incorporation, Fremont, CA.

[6] Hong Kong Government Virus Unit, Department of Health, Hong Kong Special Administrative Region, The People's Republic of China.

[7] Joint Queen Elizabeth Hospital/Hong Kong Government Virus Unit/Ciphergen Biosystems Incorporation SARS Proteomics Study Group.

†These authors contributed equally to this work.

*Address correspondence to this author at: Department of Clinical Oncology, Queen Elizabeth Hospital, 30 Gascoigne Rd., Kowloon, Hong Kong SAR. Fax 852-23594782; e-mail lawck@ha.org.hk.

Part of the data was presented in the Fourth Annual Human Proteome and Protein Chip Conference, January 12, 2004, and was granted the Best Poster Award.

Received March 12, 2004; accepted August 6, 2004.

Previously published online at DOI: 10.1373/clinchem.2004.031229

[8] Nonstandard abbreviations: CoV, coronavirus; SARS, severe acute respiratory syndrome; RT-PCR, reverse transcription-PCR; SELDI-TOF MS, surface-enhanced laser desorption/ionization time-of-flight mass spectrometry; CT, computed tomography; OGP, *N*-octyl-β-D-glucopyranoside; IMAC, immobilized metal affinity capture; SDS-PAGE, sodium dodecyl sulfate–polyacrylamide gel electrophoresis; MS/MS, tandem mass spectrometry; SAA, serum amyloid A; and IL-1 and -6, interleukin-1 and -6, respectively.

being infected and 774 deaths *(1)*. The pneumonia and accompanying adult respiratory distress syndrome can be rapidly progressive and can lead to death *(2, 3)*. The most commonly used laboratory diagnostic tests for SARS-CoV infection are reverse transcription-PCR (RT-PCR) for respiratory, rectal, or stool samples and anti-SARS-CoV antibody serologic studies *(4, 5)*, but they do not appear to have a role in monitoring pneumonia. Although serial chest radiographs are helpful for monitoring the progress of disease *(6, 7)*, more objective markers have not been well described. In this study, we analyzed the serum proteins in SARS patients by a powerful proteomics technology, surface-enhanced laser desorption/ionization time-of-flight mass spectrometry (SELDI-TOF MS) *(8–11)*, or in short, protein chip array profiling, in an attempt to identify biomarkers that were differentially increased or decreased in SARS patients and to subsequently investigate the possible roles of these biomarkers in disease monitoring.

Materials and Methods

PATIENTS AND TREATMENT PROTOCOLS

Serum samples from 28 SARS patients managed in the Department of Medicine, Queen Elizabeth Hospital, Hong Kong, were studied. The diagnoses of all patients were confirmed by a positive RT-PCR test for SARS-CoV RNA or anti-SARS-CoV antibody serologic test. The clinical pictures of this cohort of patients were similar to those reported in the literature. Most patients (87%) had abnormal chest radiographs on admission, and some (13%) presented early such that high-resolution thoracic computer tomography (CT) scanning was required to confirm the presence of pulmonary involvement. Patients were initially managed with broad-spectrum antibiotics and supportive therapy. After the diagnosis of clinical SARS was made and if there was no response to antibiotic therapy, combination therapy with ribavirin (400 mg intravenously every 8 h) and systemic steroids [intravenous hydrocortisone (200 mg) every 6–8 h or intravenous methylprednisolone ($3\ mg \cdot kg^{-1} \cdot day^{-1}$)] was initiated. The latter would be continued in a tailing manner for a total of 21 days. Intravenous pulse methylprednisolone, in a daily dose of 500 mg to 1 g for 2–3 days, would be initiated when the clinical condition, radiologic presentation, or oxygen saturation status deteriorated (at least for two of the three). The clinical characteristics, detailed management plan, and treatment regimen of this cohort of patients were described in a previous publication *(2)*.

SERUM SAMPLES

Forty-four serum samples were available from 24 SARS patients for initial expression differential mapping of serum proteins by protein chip array profiling to identify biomarkers that were differentially increased or decreased in the patients. In addition, 45 serial samples were available from four additional SARS patients with comprehensive clinical follow-up. Seventy-two sera from 51 patients suffering from infections by influenza A virus (12 sera from 6 patients), influenza B virus (8 sera from 4 patients), respiratory adenovirus (12 sera from 6 patients), respiratory syncytial virus (10 sera from 5 patients), hepatitis B virus (10 sera from 10 patients), *Mycobacterium tuberculosis* (10 sera from 10 patients), and various other bacteria (with positive bacterial culture; 10 sera from 10 patients) plus 10 sera from 10 apparently healthy individuals who attended a familial nasopharyngeal cancer screening clinic but were shown to have no malignancy served as negative controls for this study. The sera were collected and aliquoted for various routine laboratory tests. Remaining sera were kept frozen at −70 °C until protein chip array profiling analysis was performed.

SERIAL CHEST RADIOGRAPHIC SCORES

The severity and extent of pneumonia in the four SARS patients with longitudinal follow-up were assessed by a radiologist, who was "blinded" to the clinical manifestations, using a serial chest radiographic score derived initially to assess computer tomography of the chest *(6)*. Briefly, the frontal chest x-ray radiograph was divided into six lung zones (left upper zone, left middle zone, left lower zone, right upper zone, right middle zone, and right lower zone), with the upper zone representing the area above the carina (including the apex), the middle zone from the carina to the level of inferior pulmonary veins, and the lower zone from the lower margin of the middle zone to the lung base. The opacity in each lung zone was scored by a "coarse semiquantitative method" with a five-point scale of grades 0–4 representing involved areas of 0%, 5–24%, 25–49%, 50–74%, and 75–100%, respectively. The grading from each of the six lung zones was then added to provide a 0–24 point summation scale.

PROTEIN CHIP ARRAY PROFILING

The proteins in the SARS and control sera were first fractionated by use of anion-exchange Q-Hyper D ceramic resin (Ciphergen Biosystems) in 96-well silent screen filter plates (with a pore size of 0.45 μm). Briefly, the resin was prepared by washing with five bed volumes of 50 mmol/L Tris-HCl (pH 9) three times and then equilibrated in the filter plate with 200 μL/well of 50 mmol/L Tris-HCl buffer containing 1 mol/L urea and 2.2 g/L CHAPS (1 mol/L urea buffer). Sera were then removed from the −70 °C freezer and thawed, and 20 μL of each serum was denatured by adding 30 μL of 50 mmol/L Tris-HCl buffer containing 9 mol/L urea and 20 g/L CHAPS with vortex-mixing for 20 min at 4 °C. This sample mixture was then loaded in each well of the filter plate, and 50 μL of 1 mol/L urea buffer was added. The plate was shaken on an orbital shaker for 30 min at 4 °C and centrifuged, with a collection plate placed underneath, at 300*g* for 1 min to collect the flow-through fraction. We then added 100 μL of 50 mmol/L Tris-HCl buffer containing 1 g/L *N*-octyl-β-D-glucopyranoside (OGP) at pH 9 (pH 9 washing buffer) to the plate and

rinsed the resin under vigorous vortex-mixing on an orbital shaker for 10 min; the rinse was then collected by centrifugation and mixed together with the previously flow-through fraction. Fractionation was then repeated similarly with a pH 7 washing buffer (100 mmol/L sodium phosphate containing 1 g/L OGP at pH 7), a pH 5 washing buffer (100 mmol/L sodium acetate containing 1 g/L OGP at pH 5), a pH 4 washing buffer (100 mmol/L sodium acetate containing 1 g/L OGP at pH 4), a pH 3 washing buffer (50 mmol/L sodium citrate containing 1 g/L OGP at pH 3), and finally an organic washing buffer (333 mL/L isopropanol, 167 mL/L acetonitrile, and 1 mL/L trifluoroacetic acid). The six resulting serum anion-exchange fractions (F1–F6, representing the flow-through fraction at pH 9; the fractions at pH 7, pH 5, pH 4, and pH 3; and the organic fraction, respectively) were frozen at −70 °C until chip binding was initiated.

The six serum fractions were then profiled on a copper(II) immobilized metal affinity capture [IMAC Cu(II)] ProteinChip® Array and a weak cation-exchange (CM10) ProteinChip Array according to the instruction manual from Ciphergen Biosystems Incorporation. A pretreatment step is required for IMAC Cu(II) chips but not for CM10 chips. Briefly, the IMAC Cu(II) chips were loaded on a bioprocessor, and to each spot of the chips was added 50 μL of 100 mmol/L $CuSO_4$ buffer. The chips were vortex-mixed vigorously and rinsed with distilled water, after which 50 μL of 100 mmol/L sodium acetate buffer was added to the chips with strong vortex-mixing to remove the unbound copper. The chips were then rinsed with water and equilibrated with a chip binding buffer (100 mmol/L sodium phosphate buffer, pH 7, containing 0.5 mol/L NaCl). We added 80 and 90 μL of the chip binding buffer to each spot of the IMAC Cu(II) and CM10 chips, respectively; we then added 20 and 10 μL of the serum fraction to the IMAC Cu(II) and CM10 chips, respectively, followed by vigorous vortex-mixing for 30 min at room temperature. The chips were then washed twice with 150 μL of the chip binding buffer with vortex-mixing for 5 min each. They were then washed twice with 200 μL of distilled water. One microliter of an energy-absorbing molecule, sinapinic acid in 500 mL/L acetonitrile–5 mL/L trifluoroacetic acid, was applied twice to each spot, with the chip being air-dried for 10 min between applications. The chips were read in a Protein Biological System IIc mass spectrometer reader (Ciphergen Biosystems Incorporation), and the time-of-flight spectra were generated by, on average, 338 laser shots per sample. Mass accuracy was calibrated externally by use of the All-in-1 peptide molecular mass standard (Ciphergen Biosystems Incorporation). All controls were run concurrently and intermingled with the patients' samples on the same chip and on multiple chips.

Variability analyses were also performed to analyze spot-to-spot and chip-to-chip variations in the IMAC Cu(II) and CM10 chips. Briefly, reference serum samples were repeatedly bound to four different spots on four different chips, using ion-exchange serum fractions 1, 3, and 6 (F1, F3, and F6) for IMAC Cu(II) chips and fractions 1 and 4 (F1 and F4) for CM10 chips. The pooled CVs for peaks with signal-to-noise ratios >5 in the mass range of 2–200 kDa were calculated.

DATA AND STATISTICAL ANALYSES

The protein chip profiling spectra from all serum samples were collected and analyzed by Ciphergen ProteinChip Software 3.0.2 *(12)*. The mass range of 2–200 kDa was analyzed with molecules from 0 to 2000 Da being eliminated because artifacts produced by the energy-absorbing molecule and other chemical contaminants usually lie at this mass range. The peaks were baseline-subtracted, calibrated on mass accuracy, detected, and clustered automatically by the analysis software. In the Biomarker Wizard mode, the normalized peak height (or intensity) of each peak detected in sera from SARS patients was compared with that in the control groups by a nonparametric two-sample Mann–Whitney *U*-test *(13)* to identify the peaks that were significantly increased or decreased in SARS patients. Briefly, this was done by operation in two passes with the first pass detecting major well-defined peaks that were different between the SARS and control groups and the second pass defining the remaining small peaks that differed between the groups, using a criterion of a twofold or greater difference in peak height after data normalization in the two groups. The normalized peak intensities in the SARS patients with longitudinal follow-up were also correlated with the chest x-ray opacity score and other clinical manifestations.

PEPTIDE MAPPING AND TANDEM MASS SPECTROMETRY

For protein identification, we subjected fraction 1 from the ion-exchange filtrate of the SARS sera to further purification by use of immobilized copper ion spin columns (IDA-Cu Hypercel; Ciphergen Biosystems). The bound proteins were eluted by boiling in sample loading buffer for sodium dodecyl sulfate–polyacrylamide gel electrophoresis (SDS-PAGE). The eluted antigens were then resolved by SDS-PAGE in a 4–12% gradient gel (NuPAGE; Invitrogen), and a protein band at ~11.6 kDa in the gel was excised *(14)*. This protein band was then subjected to overnight tryptic digestion in a reaction volume of 20 μL of 50 mmol/L ammonium bicarbonate buffer, pH 8.0, containing 1 pmole of trypsin *(15)*. Subsequently, 2 μL of the digestion mixture was analyzed on a Normal Phase ProteinChip Array (NP20). α-Cyano-4-hydroxycinnamic acid (Ciphergen Biosystems) was used to facilitate desorption/ionization of the peptides generated from the tryptic digest. The masses of the tryptic digested peptides were measured by the ProteinChip Reader and were used for initial protein identification from the Profound database available on the internet

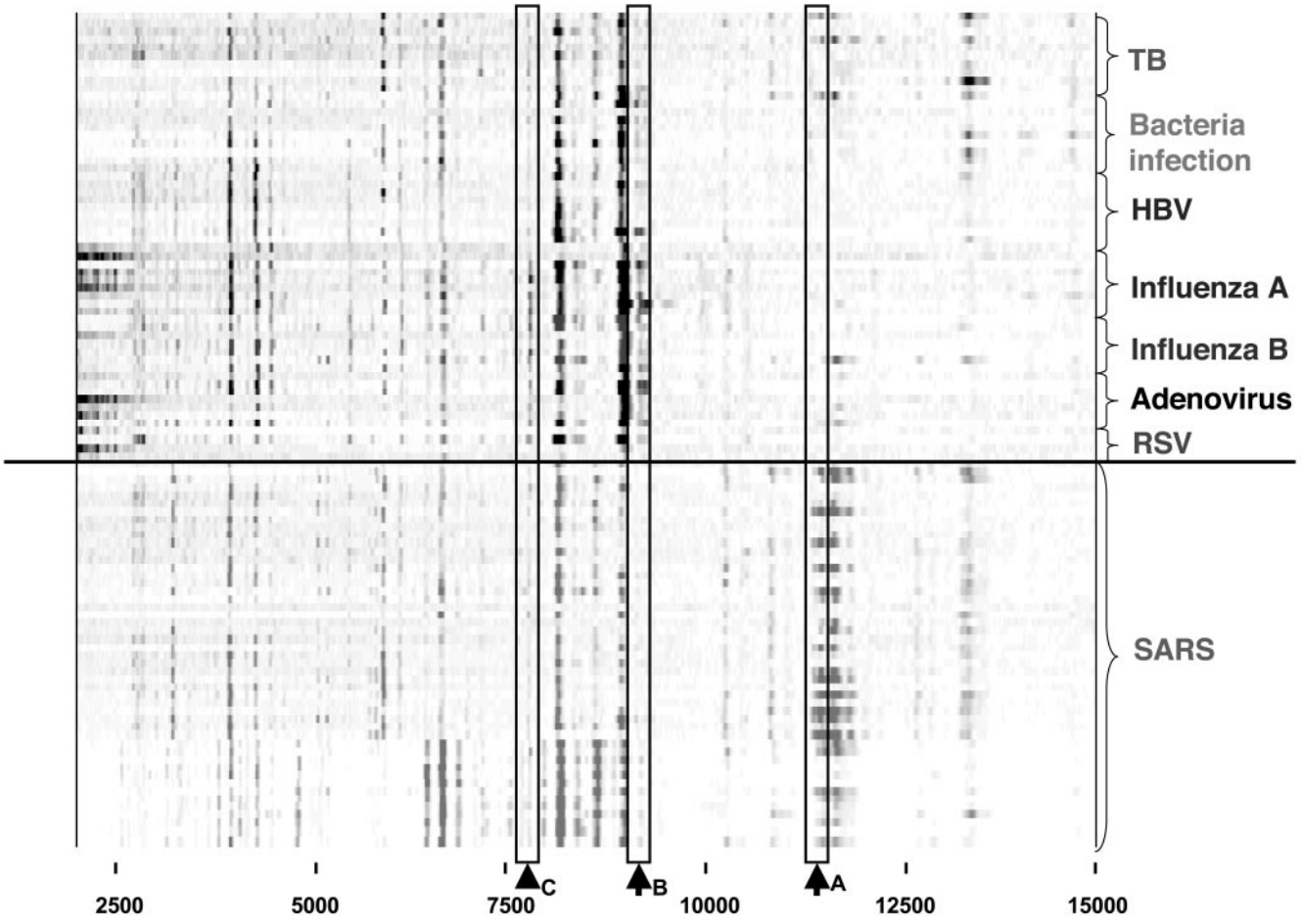

Fig. 1. Gel view of partial protein profiling results for SARS patients vs control infection groups.

Shown is part of the profiling results of fraction 1 from the ion-exchange serum filtrate in SARS patients vs the control patients in a range of molecular sizes from 2000 to 15 000 Da. *TB*, *M. tuberculosis*; *HBV*, hepatitis B virus; *RSV*, respiratory syncytial virus. The *arrows* indicate three clusters of biomarkers, *A*, *B*, and *C*, at 11 695, 9159, and 7784 Da, respectively, with cluster A being differentially increased in SARS patients and clusters B and C being differentially decreased compared with the controls.

http://prowl.rockefeller.edu/. The identity of the protein was further confirmed by tandem mass spectrometry (MS/MS) fragmentation analysis of five major peptides (at molecular masses of 1455.8, 1550.8, 1611.9, 1640.9, and 1941.1 Da) generated from the tryptic digest on a ABI Q-Star™ quadrupole tandem mass spectrometer equipped with a Ciphergen ProteinChip Interface (PCI-1000) as described previously *(16)*. Fragmentation of each peptide generated a set of MS/MS ion fingerprint, which was then entered into a mass spectrometry database search engine, Mascot (http://www.matrixscience.com/), to find the closest match with known proteins as reported previously *(17)*. A probability-based Mowse score >33 thus generated indicates that the MS/MS ion profile matched with good homology a known protein in the database with a P value <0.05, whereas a score of 90 represents matching with a known protein with almost absolute identity.

Results

PROTEIN CHIP ARRAY PROFILING ANALYSIS

More than 1000 biomarkers were resolved by protein chip array profiling of six fractions of anion-exchange filtrates from each SARS patient's serum. Fig. 1 shows the gel view of part of the profiling results for SARS patients in conjunction with the control patients in the molecular size range of 2000–15 000 Da. Three serum biomarker clusters (A, B, and C in Fig. 1) with differential expression in SARS patients vs the controls were observed, with the cluster at 11 695 Da (cluster A) being increased in SARS patients and the remaining two clusters at 9159 and 7784 Da (clusters B and C) being decreased. Analyzing the whole serum biomarker profile, we identified nine biomarkers (at molecular sizes of 4922, 5104, 5215, 5833, 10 867, 11 508, 11 695, 11 871, and 14 715 Da, respectively) that were significantly increased and three (at molecular sizes of 7784, 8416, and 9159 Da) that were significantly decreased

in SARS patients vs the control infection groups and apparently healthy individuals (Table 1). Further analysis of the distribution of the relative peak intensities of the biomarker at 11 695 Da showed significant increases in SARS patients against each individual control infection group or healthy individuals (Fig. 2).

CHIP-TO-CHIP AND SPOT-TO-SPOT VARIABILITIES

To investigate whether the protein chip profiling results were consistent and reproducible, we tested the ion-exchange fractions from a reference serum on four different spots on the same chip (for spot-to-spot variability) and on the same spot on four different chips (chip-to-chip variability; see Table 1 in the Data Supplement that accompanies the online version of this article at http://www.clinchem.org/content/vol50/issue12/). The CVs of the mean intensities of various peaks on IMAC Cu(II) chips and CM10 chips were determined. The chip-to-chip CVs for IMAC Cu(II) chips varied from 1% to 16% for the small and large mass ranges, whereas the spot-to-spot CVs varied from 1% to 14%. CM10 chips had relatively higher variabilities, with chip-to-chip CVs of 9–24% and spot-to-spot CVs of 8–26%. However, these variabilities were within a reasonable range for us to compare the peak intensities between the SARS and control groups and to correlate the peak intensities of a biomarker at 11 695 Da with clinical manifestations and radiographic scores in SARS patients.

Table 1. Serum biomarkers significantly increased or decreased in SARS patients vs seven control groups with other infections and apparently healthy individuals.

Biomarker number	Molecular size, Da	Differential expression	P^a
1	4922	Increased	1.1×10^{-4}
2	5104	Increased	7.1×10^{-8}
3	5215	Increased	6.4×10^{-4}
4	5833	Increased	3.1×10^{-9}
5	7784	Decreased	4.9×10^{-8}
6	8416	Decreased	1.6×10^{-7}
7	9159	Decreased	1×10^{-10}
8	10 867	Increased	3.6×10^{-7}
9	11 508	Increased	1.3×10^{-5}
10	11 695	Increased	5.4×10^{-6}
11	11 871	Increased	8.4×10^{-4}
12	14 715	Increased	3.9×10^{-9}

[a] *P* values were obtained by Mann–Whitney *U*-test comparing the normalized peak intensities of the biomarkers in 44 sera from 24 SARS patients vs those in 72 sera from 51 patients in seven control infection groups (12 sera from 6 patients with influenza A virus infections, 8 sera from 4 patients with influenza B infections, 12 sera from 6 patients with respiratory adenovirus infections, 10 sera from 5 patients with respiratory syncytial virus infections, 10 sera from 10 patients with hepatitis B virus infections, 10 sera from 10 patients with *M. tuberculosis* infections, 10 sera from 10 patients with positive bacterial cultures) and 10 sera from 10 apparently healthy individuals attending a familial cancer screening clinic.

PROTEIN IDENTIFICATION

To characterize the nature of the biomarker at 11 695 Da, we subjected the protein band at ~11.7 kDa, as resolved by SDS-PAGE, to tryptic digestion to generate a series of peptide fragments (Fig. 3A). When we submitted these peptide fragments to the Profound database search engine, it matched with 100% probability to human serum amyloid A protein (SAA) as the first choice. SAA had a matching probability of 1, with the second choice, a human hypothetical protein (XP_299056), having a probability of 8.9×10^{-6}. To further confirm the identity of SAA, we performed separate fragmentation analyses, in a tandem mass spectrometer, on each of the five peptides generated by the tryptic digestion of the 11.7-kDa protein. Shown in Fig. 3B is one MS/MS ion fingerprint generated from the peptide at 1550.8 Da (Fig. 3A). When we entered the ion fingerprint from this peptide into a mass spectrometry search engine database, Mascot, it gave a Mowse score of 90, which indicated almost absolute identity with human SAA, further confirming the tryptic mapping findings. Ion fingerprints from the remaining four peptides also confirmed SAA as the predominant protein (data not shown).

LONGITUDINAL FOLLOW-UP OF SERUM SAA IN SARS PATIENTS

With SAA being identified as one of the predominantly increased biomarkers in SARS patients, we correlated its concentrations with the clinical findings and serial chest radiographic scores in four SARS patients as follows:

SARS patients 1–4 under longitudinal follow-up. After SARS-CoV infection was diagnosed, the radiographic score of the first patient under longitudinal follow-up started to increase from a value of 6 to a peak of 16 and then gradually decreased to 12, 9, and finally to 4, demonstrating a progressive recovery (Fig. 1 in the online Data Supplement). The SAA concentration by protein chip profiling showed an increase that peaked earlier than the radiographic score but then also gradually decreased along with the radiographic score to a nadir when the patient was discharged.

The second patient had clinical SARS symptoms with the SARS-CoV infection subsequently confirmed by RT-PCR. On treatment, her radiographic score remained high initially but then decreased with her progressive recovery (Fig. 2 in the online Data Supplement). Protein chip profiling also revealed that the SAA concentration increased initially but soon decreased similarly to the radiographic score. The SAA peak also preceded the score.

The third patient had typical clinical SARS symptoms with the viral disease confirmed by paired serum anti-SARS-CoV antibody tests performed twice. The clinical course after treatment was uneventful with a low radiographic score, which later decreased to zero. The SAA concentration was low throughout the monitoring period (Fig. 3 in the online Data Supplement).

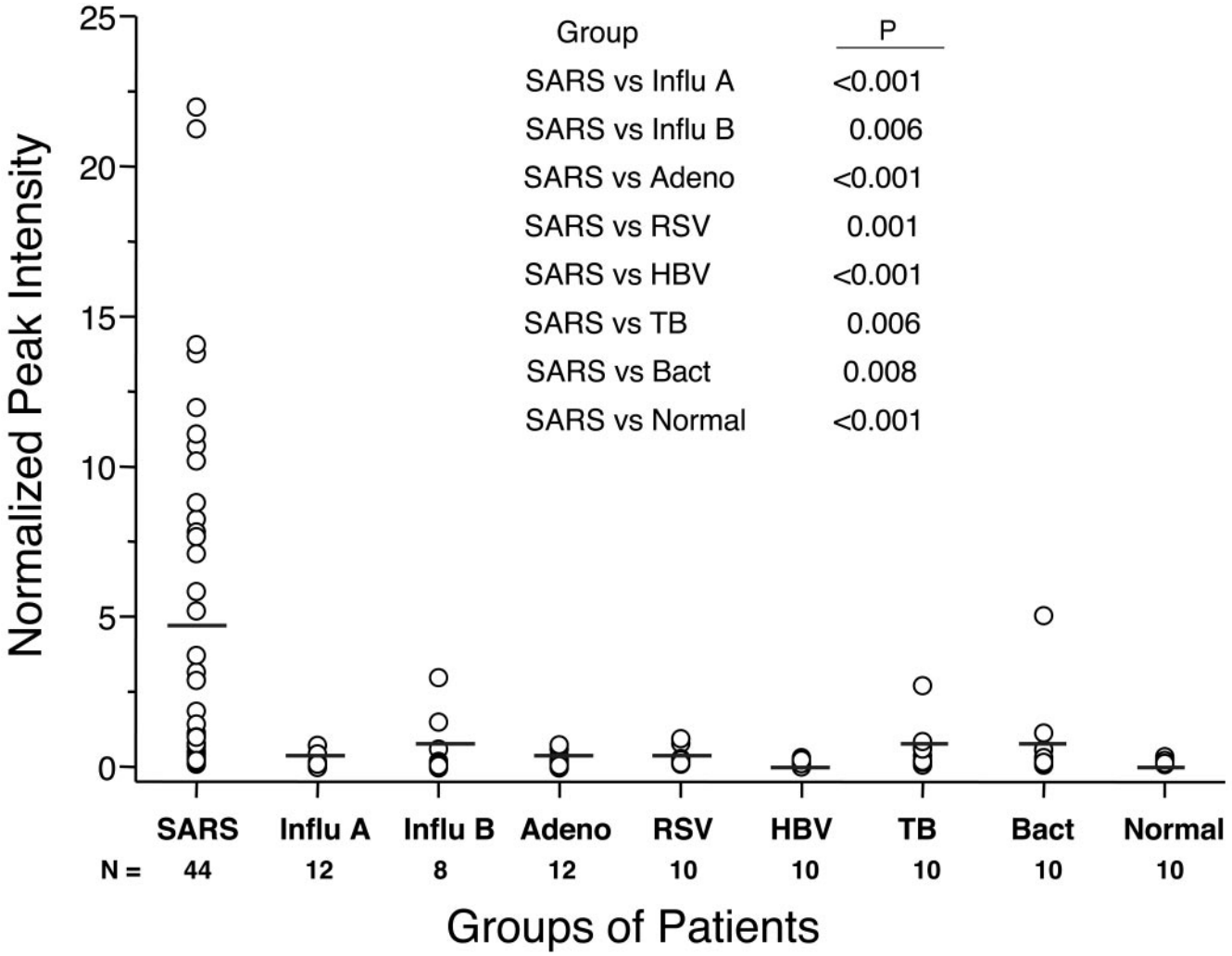

Fig. 2. Distribution of normalized peak intensities of the biomarker at 11 695 Da in sera from SARS patients and control groups after protein chip array profiling analysis.

The normalized peak intensities of this marker in sera from SARS patients were compared with those of the other seven control infection groups and the apparently healthy individuals by Mann–Whitney *U*-test. A *P* value ≤0.05 indicates a statistically significant difference between the two groups. *Influ A*, influenza A virus infection; *Influ B*, influenza B virus infection; *Adeno*, adenovirus infection; *RSV*, respiratory syncytial virus infection; *HBV*, hepatitis B virus infection; *TB*, *M. tuberculosis* infection; *Bact*, bacterial culture positive; *Normal*, apparently healthy individuals.

Despite treatment, the pneumonic condition of the fourth patient remained severe, with high radiographic scores after 3 days of treatment. Her SAA concentrations began to increase as well and were further increased on diagnosis of superimposed bacterial infections (Fig. 4 in the online Data Supplement). A subsequent decrease in the SAA concentration was observed after initiation of antibiotic treatment, although it remained significantly increased thereafter. The patient still harbored the virus as indicated by positive RT-PCR from various sources. The radiographic score remained high until she later died of the disease.

Discussion

Conventional CoV usually causes mild and self-limiting cold-like symptoms but rarely severe lower respiratory tract infection *(18)*. In contrast, SARS-CoV can give rise to rapidly progressing pneumonia and can be associated with a significantly high mortality rate *(2, 3)*. Most SARS patients develop pulmonary infiltrates within 48 h of onset of disease *(19)*, usually in the form of focal and unilateral consolidation in the peripheral regions of the lung *(20)*. The consolidation usually clears quickly, but a small proportion of patients progress to bilateral consolidation with extensive pneumonic involvement and protracted clinical course *(7)*. Serial chest radiographs are helpful in the diagnosis and monitoring of the clinical course *(6, 7)*, but their interpretation can be confounded by a lack of available experienced radiologists, by inter-observer variability, and by the frequently suboptimal quality of portable films taken in isolation wards to avoid the spread of infections to other patients.

SARS-CoV antibody is usually increased at a later stage of disease *(21)* and is therefore not a good marker for

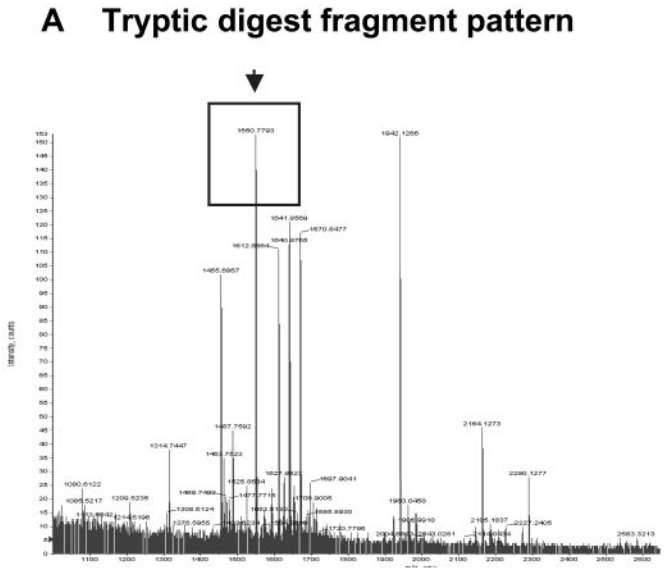

Rank	Probability	Protein Information	Mass,kDa
1	1.0	Amyloid related serum protein SAA [Homo sapiens]	11.66
2	8.9×10^{-6}	Hypothetical protein XP_ 299056 [Homo sapiens]	39.3

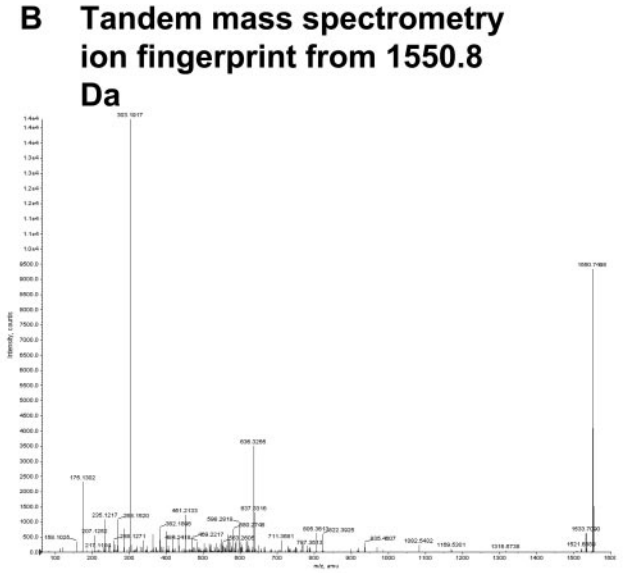

Mowse Score	Protein Information	Mass,kDa
90	Amyloid related serum protein SAA [Homo sapiens]	11.66

Fig. 3. Identification of the biomarker at 11 695 Da as SAA protein by peptide mapping followed by MS/MS analysis.

IDA-Cu spin column separation followed by SDS-PAGE of fraction 1 from the ion-exchange filtrates resolved a protein band at ~11.6 kDa. This band was excised and produced a pattern of digested fragments as illustrated in *A*. SAA was identified as the most likely biomarker by the Profound database search engine (http://prowl.rockefeller.edu/) with a probability of 1.0, with the second choice of biomarker having a much lower probability (8.9×10^{-6}). Five major peptides at 1455.8, 1550.8, 1611.9, 1640.9, and 1941.0 Da generated from the tryptic digest of the protein at 11 695 Da were subjected to MS/MS fragmentation analyses. A set of ion fingerprints produced from the peptide at 1550.8 Da is shown in *B*. A high Mowse score of 90 was generated by this peptide and the four remaining ones, indicating a match with SAA in absolute identity (a Mowse score >33 illustrates good homology at a *P* value <0.05).

monitoring the extent of disease. With a high titer being predictive of the need for intensive care, it has been suggested that quantitative real-time RT-PCR to determine the viral load *(22)* may have prognostic value *(23)*. However, its use in monitoring the disease is probably limited or at least unclear because the lung damage in SARS appears to be more related to immunopathologic consequences of host response than to virus replication *(22)*. It has also been suggested that lymphopenia or T-cell lymphopenia, a fairly common occurrence in SARS patients *(24, 25)*, might potentially be a marker for disease activity. However, the presence of other superimposed viral or bacterial infections, as well as the effects of treatment with steroids and intravenous immunoglobulins, might also affect the lymphocyte counts, making them less ideal for monitoring the disease activity of SARS.

A high serum lactate dehydrogenase concentration has been reported to be associated with an adverse patient outcome *(26)* with concentrations peaking at the height of the disease and decreasing to within reference values on remission and after discharge *(27)*. Because this enzyme can originate from many sources, such as the heart, skeletal muscles, erythrocytes, and liver, its increase might also be attributable to disease conditions in these organs or disease complications such as rhabdomyolysis *(28)* and hemolytic anemia after ribavirin treatment *(27, 29)*. Hence, a change in lactate dehydrogenase activity might not be specific enough for monitoring the disease.

Modern mass spectrometry has revolutionized proteomics studies by enabling rapid resolution of >1000 biomarkers from a single serum sample. A large number of samples can also be processed within a short period of time. SELDI-TOF MS, or protein chip profiling, has further advanced the technology by combining mass spectrometry with a surface-enhanced biochip, which allows uniform and reproducible binding and desorption of biomarkers so that quantitative comparison of individually resolved biomarkers in serially monitored patients is possible *(8, 10)*. Using this profiling technology, we found at least 12 serum biomarkers that were differentially increased or decreased in SARS patients. Among them, an acute-phase protein, SAA, was substantially increased in 44 sera from 24 SARS patients, in contrast to 72 sera from 51 control patients with different viral or bacterial infec-

tions. Using a clinically useful chest radiographic score, we found that the SAA concentration correlated well with the extent of pneumonia in four patients for whom serial serum samples were available. In the first two patients, this protein was increased, similar to the increase in radiographic score in the active phase of the disease within the first 2 weeks of symptom onset. The slightly earlier peaks in SAA concentrations compared with the radiographic scores could perhaps indicate that SAA might be an earlier marker in disease activity, although this requires further validation. In the third patient, who had a milder disease course and lesser extent of pneumonic involvement, SAA concentrations remained relatively low throughout, indicating that this biomarker correlates well with the severity of disease.

As an acute-phase protein synthesized by the liver, SAA has been reported to be increased in infectious and arthritic diseases *(30–32)* and malignancies *(33)*. The increase has been found to be more prominent in some bacterial infections than in non-SARS-CoV viral infections *(30)*. Hence, it is not surprising that the fourth patient demonstrated an increase in SAA concentration in the near-terminal part of her illness when there were superimposed bacterial infections, followed by a slight decrease after antibiotics were initiated. This increase was probably additional to the persistent SARS-CoV infection, as demonstrated by the persistently positive RT-PCR results for samples from various sources and her continuous severe radiologic abnormalities. Such an increase in SAA was, however, in contrast to the low concentrations of this protein in the tested control viral and bacterial infections (Figs. 2 and 3) and probably was a result of the severity of multiple superimposed infections and septicemia in this patient. Secondary severe bacterial infection, which can cause high mortality, is not uncommon in SARS patients with pneumonia; therefore, increased SAA concentrations in the presence of severe secondary infections in SARS patients could be an advantage rather than a disadvantage if the aim is to monitor patients for severity of disease.

Apart from SAA, other candidate acute-phase proteins, such as α_1-acid glycoprotein, α_1-antitrypsin, haptoglobulin, and C-reactive protein, exist in various mammals *(34, 35)*. SAA was found to be more sensitive than C-reactive protein in detecting minor inflammatory stimuli in certain viral infections *(30)* and in noninvasive and early invasive bacterial infections *(31)*. A study of feline disease conditions also showed that SAA was the earliest marker induced when compared with α_1-acid glycoprotein, haptoglobulin, and C-reactive protein *(35)*. This lends support to the possibility that SAA might also manifest earlier than the radiographic score, although this remains to be confirmed in subsequent studies.

Despite various reports on the potential applications of SELDI-TOF MS for the diagnosis of various diseases, this technology has also been suggested to only detect high-abundance proteins such as acute-phase reactants *(36–38)*. As far as the SARS-CoV infection is concerned, the major mortality-causing symptom is pneumonia; therefore, the discovery of acute-phase proteins that are strongly associated with pneumonia-related inflammatory events is expected and entirely matches with the theme of this study in pneumonia monitoring. Although the individual acute-phase proteins detected in this study may not be absolutely specific to SARS-CoV infection per se, our preliminary data showed that the SELDI analysis showing a distinctive pattern of increase and decrease of these proteins and their variants can distinguish SARS from other infectious respiratory diseases very well (data not shown).

The precise mechanism for the increase of SAA concentrations in SARS patients remains to be investigated. Pulmonary infiltrates and acute-phase diffuse alveolar damage were frequently found in the SARS patients *(39, 40)*. It is also widely known that such infiltrates and diffuse alveolar damage can serve as stimuli for the production and secretion of a variety of inflammatory cytokines. SARS patients have been shown to have markedly increased plasma concentrations of two inflammatory cytokines, interleukin-1 (IL-1) and IL-6 *(41)*. Knowing that IL-1 and IL-6 can rapidly induce 1000-fold increases in SAA in a synergistic manner *(42)*, it thus perhaps explains the possible rapid induction of this acute-phase reactant at the time of SARS CoV infection. With the encouraging correlation of SAA concentration with the extent of pneumonia and the possible correlation of increases or decreases in the remaining serum biomarkers with disease conditions as well, SAA and probably the other biomarkers discussed could be used to monitor disease activity and response to treatment in SARS patients.

We thank our Kowloon Central Cluster/Queen Elizabeth Hospital Chief Executive, Dr. Lawrence Lai, and the SARS Management Committee for their support in this project. We also express our appreciation to K.H. Leung, C.C. Tiu, Gene G.T. Lau, Dr. Cesar S.C. Wong, and Elena S.F. Lo in the Pathology Department of Queen Elizabeth Hospital for their help in collecting all of the sera used in this study. This work was supported in part by grants from Queen Elizabeth Hospital and the Hong Kong Jockey Club.

References

1. World Health Organization. WHO issued consensus document on the epidemiology of SARS. Wkly Epidemiol Rec 2003;78:373–5.
2. Chan JWM, Ng CK, Chan YH, Mok TYW, Lee S, Chu SY, et al. Short term outcome and risk factors for adverse clinical outcomes in adults with severe acute respiratory syndrome (SARS). Thorax 2003;58:686–9.
3. Donnelly CA, Ghani AC, Leung GM, Hedley AJ, Fraser C, Riley S, et al. Epidemiological determinants of spread of casual agent of severe acute respiratory syndrome in Hong Kong. Lancet 2003; 361:1761–6.

4. Yam WC, Chan KH, Poon LL, Guan Y, Yuen KY, Seto WH, et al. Evaluation of reverse transcriptase-PCR assays for rapid diagnosis of severe acute respiratory syndrome associated with a novel coronavirus. J Clin Microbiol 2003;41:4521–4.
5. Poon LLM, Wong OK, Luk W, Yuen KY, Peiris JSM, Guan Y. Rapid diagnosis of a coronavirus associated with severe acute respiratory syndrome (SARS). Clin Chem 2003;49:953–5.
6. Ng CS, Desai SR, Rubens MB, Padley SPG, Wells AU, Hansell DM. Visual quantitation and observer variation of signs of small airways disease at inspiratory and expiratory CT. J Thorac Imag 1999;14:279–85.
7. Grinblat L, Shulman H, Glickman A, Matukas L, Paul N. Severe acute respiratory syndrome: radiographic review of 40 probable cases in Toronto, Canada. Radiology 2003;228:802–9.
8. Fung ET, Thulasiraman V, Weinberger SR, Dalmasso EA. Protein biochips for differential profiling. Curr Opin Biotechnol 2001;12: 65–9.
9. Wright GL Jr. SELDI proteinchip MS: a platform for biomarker discovery and cancer diagnosis. Expert Rev Mol Diagn 2002;2: 549–63.
10. Issaq HJ, Veenstra TD, Conrads TP, Felschow D. The SELDI-TOF MS approach to proteomics: protein profiling and biomarker identification. Biochem Biophys Res Commun 2002;292:587–92.
11. Weinberger SR, Dalmasso EA, Fung ET. Current achievements using ProteinChip Array technology. Curr Opin Chem Biol 2002;6: 86–91.
12. Fung E, Enderwich C. ProteinChip® clinical proteomics: computational challenges and solutions. Comput Proteomics Suppl 2002; 32:S34–41.
13. Krauth J. The interpretation of significance tests for independent and dependent samples. J Neurosci Methods 1983;9:269–81.
14. Cleveland DW, Fischer SG, Kirschner MW, Laemmli UK. Peptide mapping by limited proteolysis in sodium dodecyl sulfate and analysis by gel electrophoresis. J Biol Chem 1977;252:1102–6.
15. Baudys M, Foundling S, Pavlik M, Blundell T, Kostka V. Protein chemical characterization of *Mucor pusillus* aspartic proteinase amino acid sequence homology with the other aspartic proteinases disulfide bond arrangement and site of carbohydrate attachment. FEBS Lett 1988;235:271–4.
16. Fournier I, Chaurand P, Bolbach G, Lutzenkirchen F, Spengler B, Tabet JC. Sequencing of a branched peptide using matrix-assisted laser desorption/ionization time-of-flight mass spectrometry. J Mass Spectrom 2000;35:1425–33.
17. Perkins DN, Pappin DJ, Creasy DM, Cottrell JS. Probability-based protein identification by searching sequence databases using mass spectrometry data. Electrophoresis 1999;20:3551–67.
18. Engel JP. Viral upper respiratory infections. Semin Respir Infect 1995;10:3–13.
19. Xue X, Gao Z, Xu Y, Ding X, Yuan L, Li W, et al. Clinical analysis of 45 patients with severe acute respiratory syndrome. Chin Med J (Engl) 2003;116:819–22.
20. Muller NL, Ooi GC, Khong PL, Nicolaou S. Severe acute respiratory syndrome: radiographic and CT findings. AJR Am J Roentgenol 2003;181:3–8.
21. Xu G, Lu H, Li J, Li Y, Feng Z, Hou N, et al. Primary investigation on the changing mode of plasma specific IgG antibody in SARS patients and their physicians and nurses. Beijing Da Xue Xue Bao 2003;35(Suppl):23–5.
22. Peiris JS, Chu CM, Cheng VC, Chan KS, Hung IF, Poon LL, et al. Clinical progression and viral load in a community outbreak of coronavirus-associated SARS pneumonia: a prospective study. Lancet 2003;361:1767–72.
23. Ng EK, Hui DS, Chan KC, Hung EC, Chiu RW, Lee N, et al. Quantitative analysis and prognostic implication of SARS coronavirus RNA in the plasma and serum of patients with severe acute respiratory syndrome. Clin Chem 2003;49:1976–80.
24. Wong RS, Wu A, To KF, Lee N, Lam CW, Wong CK, et al. Haematological manifestations in patients with severe acute respiratory syndrome: retrospective analysis. BMJ 2003;326: 1358–62.
25. Cui W, Fan Y, Wu W, Zhang F, Wang JY, Ni AP. Expression of lymphocytes and lymphocyte subsets in patients with severe acute respiratory syndrome. Clin Infect Dis 2003;37:857–9.
26. Lee N, Hui D, Wu A, Chan P, Cameron P, Joynt GM, et al. A major outbreak of severe acute respiratory syndrome in Hong Kong. N Engl J Med 2003;348:1984–94.
27. Avendano M, Derkach P, Swan S. Clinical course and management of SARS in health care workers in Toronto: a case series. CMAJ 2003;168:1649–60.
28. Wang JL, Wang JT, Yu CJ, Chen YC, Hsueh PR, Hsiao CH, et al. Rhabdomyolysis associated with probable SARS. Am J Med 2003;115:421–2.
29. McCromick JB, King IJ, Webb PA, Scribner CL, Craven RB, Johnson KM, et al. Lassa fever. Effective therapy with ribavirin. N Engl J Med 1986;314:20–6.
30. Nakayama T, Sonoda S, Urano T, Yamada T, Okada M. Monitoring both serum amyloid protein A and C-reactive protein as inflammatory markers in infectious diseases. Clin Chem 1993;39:293–7.
31. Lannergard A, Larsson A, Kragsbjerg P, Friman G. Correlations between serum amyloid A protein and C-reactive protein in infectious diseases. Scand J Clin Lab Invest 2003;63:267–72.
32. Cunnate G, Grehan S, Geoghegan S, McCormack C, Shields D, Whitehead AS, et al. Serum amyloid A in the assessment of early inflammatory arthritis. J Rheumatol 2000;27:58–63.
33. Cho WCS, Yip TTC, Yip C, Yip V, Thulasiraman V, Ngan RKC, et al. Identification of serum amyloid A protein as a potentially useful biomarker to monitor relapse of nasopharyngeal cancer by serum proteomic profiling. Clin Cancer Res 2004;10:43–52.
34. Yiangou M, Paraskeva E, Hsieh CC, Markou E, Victoratos P, Scouras Z, et al. Induction of a subgroup of acute phase protein genes in mouse liver by hyperthermia. Biochim Biophys Acta 1998;1396:191–206.
35. Kajikawa T, Furuta A, Onishi T, Tajima T, Sugii S. Changes in concentrations of serum amyloid A protein, α1-acid glycoprotein, haptoglobin, and C-reactive protein in feline sera due to induced inflammation and surgery. Vet Immunol Immunopathol 1999;68: 91–8.
36. Diamandis EP. Point: proteomic patterns in biological fluids: do they represent the future of cancer diagnostics? Clin Chem 2003;49:1272–8.
37. Diamandis EP. Analysis of serum proteomic patterns for early cancer diagnosis: drawing attention to potential problems. J Natl Cancer Inst 2004;96:353–6.
38. Diamandis EP. Mass spectrometry as a diagnostic and a cancer biomarker discovery tool. Mol Cell Proteomics 2004;3:367–78.
39. Franks TJ, Chong PY, Chui P, Galvin JR, Lourens RM, Reid AH, et al. Lung pathology of severe acute respiratory syndrome (SARS): a study of 8 autopsy cases from Singapore. Hum Pathol 2003;34: 743–8.
40. Nicholls JM, Poon LL, Lee KC, Ng WF, Lai ST, Leung CY, et al. Lung pathology of fatal severe acute respiratory syndrome. Lancet 2003;361:1773–8.
41. Wong CK, Lam CW, Wu AK, Ip WK, Lee NL, Chan IH, et al. Plasma inflammatory cytokines and chemokines in severe acute respiratory syndrome. Clin Exp Immunol 2004;136:95–103.
42. Uhlar CM, Whitehead AS. Serum amyloid A, the major vertebrate acute-phase reactant. Eur J Biochem 1999;265:501–23.